LA-UR-15-20242
Approved for public release; distribution is unlimited.

Title: Differential Die-Away Instrument: Report on Comparison of Fuel Assembly Experiments and Simulations

Author(s):
Goodsell, Alison Victoria
Henzl, Vladimir
Swinhoe, Martyn Thomas
Rael, Carlos D.
Desimone, David J.

Intended for: Report

Issued: 2015-01-14

Differential Die-Away Instrument: Report on Comparison of Fuel Assembly Experiments and Simulation

Alison Goodsell, Vladimir Henzl, Martyn Swinhoe, Carlos Rael, Dave Desimone

Abstract

Experimental results of the assay of mock-up (fresh) fuel with the differential die-away (DDA) instrument were compared to the Monte Carlo N-Particle eXtended (MCNPX) simulation results. Most principal experimental observables, the die-away time and the integral of the DDA signal in several time domains, have been found in good agreement with the MCNPX simulation results. The remaining discrepancies between the simulation and experimental results are likely due to small differences between the actual experimental setup and the simulated geometry, including uncertainty in the DT neutron generator yield. Within this report we also present a sensitivity study of the DDA instrument which is a complex and sensitive system and demonstrate to what degree it can be impacted by geometry, material composition, and electronics performance.

I. Introduction

The differential die-away instrument (DDA) is an active neutron interrogation system using a deuterium-tritium (DT) neutron generator to characterize properties of spent fuel assemblies (SFAs) for nuclear safeguards applications. Currently, fresh fuel measurements and MCNPX simulations are underway at LANL funded by the Defense Nuclear Nonproliferation Research and Development (DNN-RD) in support of the Next Generation Safeguards Initiative (NGSI) spent fuel DDA project. The ability to accurately model the experimental measurements using MCNPX is critical for the advancement of the DDA instrument. By using fresh fuel, we provide useful information for the development and deployment phases of a DDA instrument for the assay of spent nuclear fuel.

II. Fresh Fuel Experimental Components

2.1 Upgrade of the DDA Instrument Setup

This is the second year of the DNN-RD (WMS) funded project. In the first year, the system had been set up to provide a test of the generator, data acquisition system, and provide preliminary results. The primary objective of the DDA instrument setup upgrade was to move the DT neutron generator into the water tank to better mimic a spent fuel cooling pool environment, and to better fix the experimental component positions relative to each other (Fig. 1). A base template made of high-density polyethylene (HDPE) was designed and manufactured at LANL to precisely position the fresh fuel assembly, three stainless steel detector pods, and allow for three different positions of DT neutron generator waterproof pipe in the water tank (Fig 2). A second spacer template was used inside of the three stainless steel detectors pods to fix the position of Cd-wrapped HDPE cylinders surrounding the ^{3}He detectors (Fig. 2). We designed this cylinder template to allow for a variety of Cd-wrapped poly cylinder dimensions.

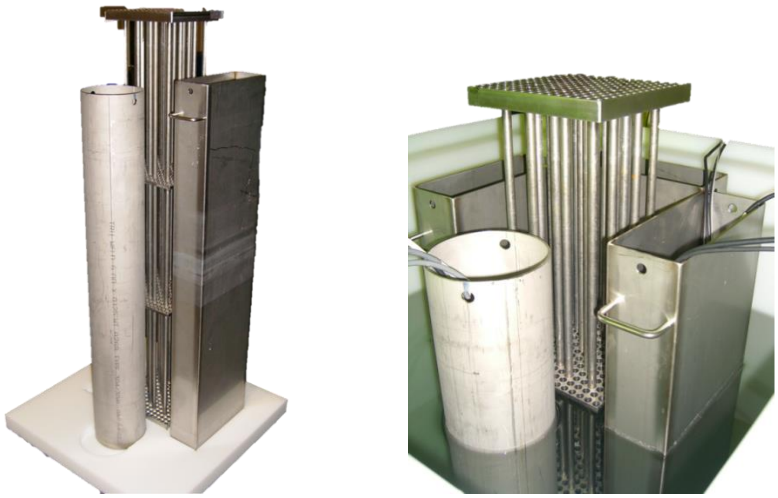

Figure 1. The upgraded DDA instrument setup with the experimental components slotted into the base template (left) and the setup submerged in the water tank (right).

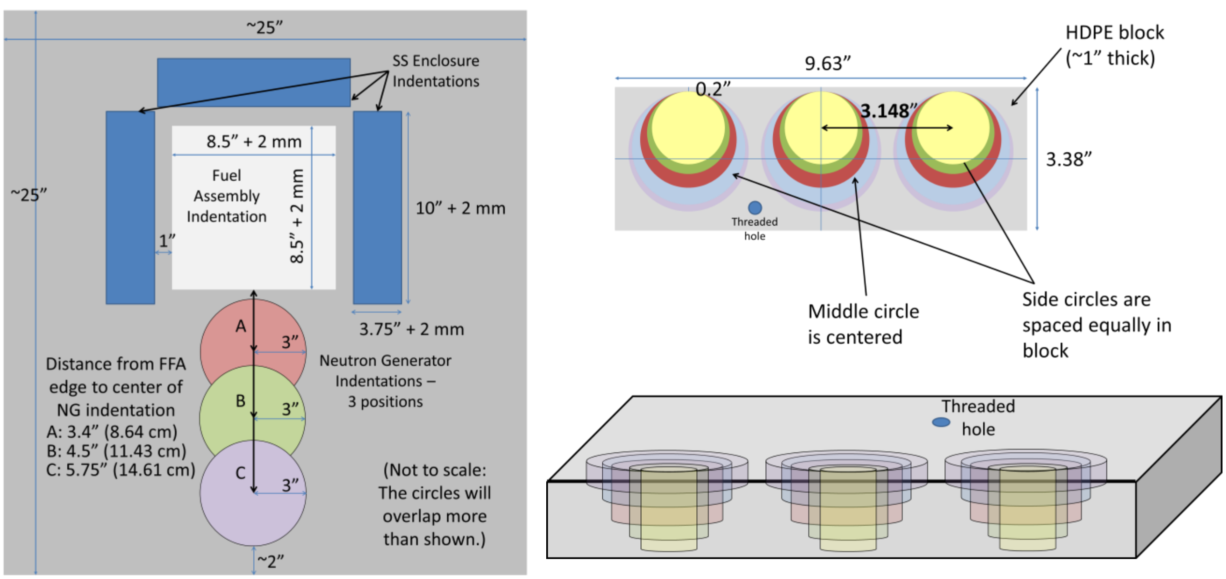

Figure 2. (Left) The upgraded DDA instrument setup is fixed in place using a HDPE base template, with slots for the FFA, three stainless steel detector pods, and neutron generator tube. (Right) Inside of the stainless steel pods, the HDPE cylinders around the detectors are set into cylindrical spacers made from HDPE.

2.2 Fresh Fuel Description

Fresh uranium dioxide (UO_2) fuel was used for the experimental assay with the DDA instrument. The fresh fuel and pressurized water reactor (PWR) assembly specifications are provided in Table I. The fresh fuel assembly (FFA) is a standard PWR 15x15 lattice with 204 fuel pin slots and 21 guide tube slots. The LANL low-enriched uranium (LEU) and depleted uranium (DU) fresh fuel pins have an average enrichment of 3.19% and 0.22% ^{235}U, respectively.

Table I

LANL PWR 15x15 fresh fuel and assembly specifications

PWR Assembly		
Lattice geometry	15 x 15	
Assembly width	21.5 cm	
Fuel pin pitch	1.4 cm	
Number of fuel pin slots	204	
Number of guide tube slots	21	
Fuel Pin Information		
Fuel type	UO_2	
Cladding type	Zircaloy-2	
Average LEU rod enrichment	3.19% ^{235}U	
Average DU rod enrichment	0.22% ^{235}U	
Fuel pellet density	10.48 g/cm^3	
Fuel pellet radius	0.4525 cm	
Cladding thickness	0.0875 cm	
Outer pin diameter	0.54 cm	
Total fuel rod length	130 cm	
Active fuel length		
LEU rod	102 cm	
DU rod	120 cm	
Inert fuel regions	LEU	DU
Top	17 cm	6 cm
Bottom	12 cm	5 cm

2.3 DT Neutron Generator

The Thermo Scientific P 385 DT neutron generator has an approximate maximum yield of $5 \cdot 10^8$ n/s of 14.1 MeV neutrons from deuterium-tritium fusion. We operate the neutron generator within the range of standard operating parameters. Our standard operating parameters are 125 kV or 90 kV, 70 μA, 10% duty cycle, and 2500 Hz pulse frequency. The neutron generator output is continually monitored by a ^3He flux monitor positioned outside of the water tank. Measurements from the flux monitor are compared between experimental campaigns to check the consistency of the neutron generator output.

2.4 Detectors and Electronics

The fresh fuel DDA project has leveraged funding from other NNSA-funded detector and electronics development projects [1]. In particular, we have tested the LANL designed and built KM200 pre-amplifier [2] and the pre-amplifiers procured for the Differential Die-Away Self Interrogation (DDSI) instrument.

For the benchmarking efforts detailed in this report, we used the DDSI pre-amplifiers, a PDT-10A with an AMPTEK A-111 chip for faster pulse processing [3]. In the future, we intend to test and develop the DDA instrument with the LANL-made KM200 pre-amplifier packages.

2.5 List-Mode Data Acquisition System

A list-mode data acquisition system, nicknamed ARIEL, was assembled at LANL using all commercially available parts. ARIEL is a rugged and portable system with 6 TB of data storage. List-mode data acquisition and analysis software was also designed at LANL for the fresh fuel DDA project.

III. Fresh Fuel Experiments

3.1 Estimation of the Uncertainty of Die-Away Times

We estimate the uncertainty of the experimentally determined die-away times by recording 10 measurements of 30 s each for three fresh fuel assemblies with different uranium enrichments (1.67%, 1.08%, and 0.49% ^{235}U) and the empty assembly without any fuel pins, when the die-away time magnitude depends on the detector system properties. For each of these 10 measurements, we determined the die-away time in the 100-200 μs time domain. The average die-away time value, standard deviation of the mean, and relative uncertainty were determined for the four cases. Overall, within the set of 10 measurements the experimental die-away times were found to be very similar, with the die-away time values generally deviating by less than 0.5 μs from the mean. The relative uncertainty in the die-away time increased marginally as the amount of fissile mass decreased. The results are provided in Table II. Based on these results, we conclude that measurement time of 30 s is sufficient for an accurate die-away time determination.

Table II

The results of ten 30 s measurements: the die-away time in the 100-200 μs time domain, the mean value, standard deviation, and relative uncertainties were determined for three fresh fuel cases (1.67%, 1.08%, and 0.49%) and the empty setup. The relative error gradually increased as the amount of fissile mass decreased.

	Die-Away Time [μs]			
	Average Enrichment (% ^{235}U)			
Run	1.67%	1.08%	0.49%	Empty
1	102.03	81.75	61.13	32.24
2	102.50	82.13	61.29	32.79
3	101.38	81.34	60.44	32.74
4	101.84	82.30	61.25	32.63
5	101.92	82.17	61.35	32.40
6	102.17	82.00	61.18	32.22
7	101.85	81.85	61.05	32.55
8	101.85	81.63	61.26	32.41
9	102.05	81.42	61.21	32.45
10	101.43	82.33	61.27	32.24
Mean	101.90	81.89	61.14	32.47
σ [μs]	0.33	0.35	0.26	0.21
σ [%]	0.3%	0.4%	0.4%	0.6%

3.2 Deadtime Correction

The approximate deadtime of the electronics had been previously determined [1]. Small changes were made to the deadtime correction coefficient to determine the impact on the calculated die-away time in two different time domains: 60-100 μs and 100-150 μs. The deadtime correction coefficient was set as 800 ns, 850 ns, and 900 ns. The die-away time of the DDA signal was determined at these three values for several FFA enrichments. (For more information on the DDA electronics deadtime correction method, see the previous reference.)

We found that in the early time domain (60-100 μs), Detectors 1 and 2 were particularly sensitive to the correction factor. Detectors in the positions farther from the DT neutron generator (and therefore experiencing lower count rates) were less affected (Fig. 3A). As we changed the correction coefficient from 900 ns to 800 ns in intervals of 50 ns, the measured die-away time for all detectors increased by approximately:

- Higher enriched cases: 4-7 μs for the front detectors, 1-2 μs for the back detectors
- Lower enriched cases: 1-3 μs for the front detectors, 0-0.75 μs for the back detectors

For the later time domain (100-150 μs), we found the detectors were not nearly as sensitive to the deadtime correction coefficient (Fig. 3B). However, there was still a small range in the determined die-away times which should be considered when comparing experimental data to simulation results, as MCNPX simulations do not include deadtime.

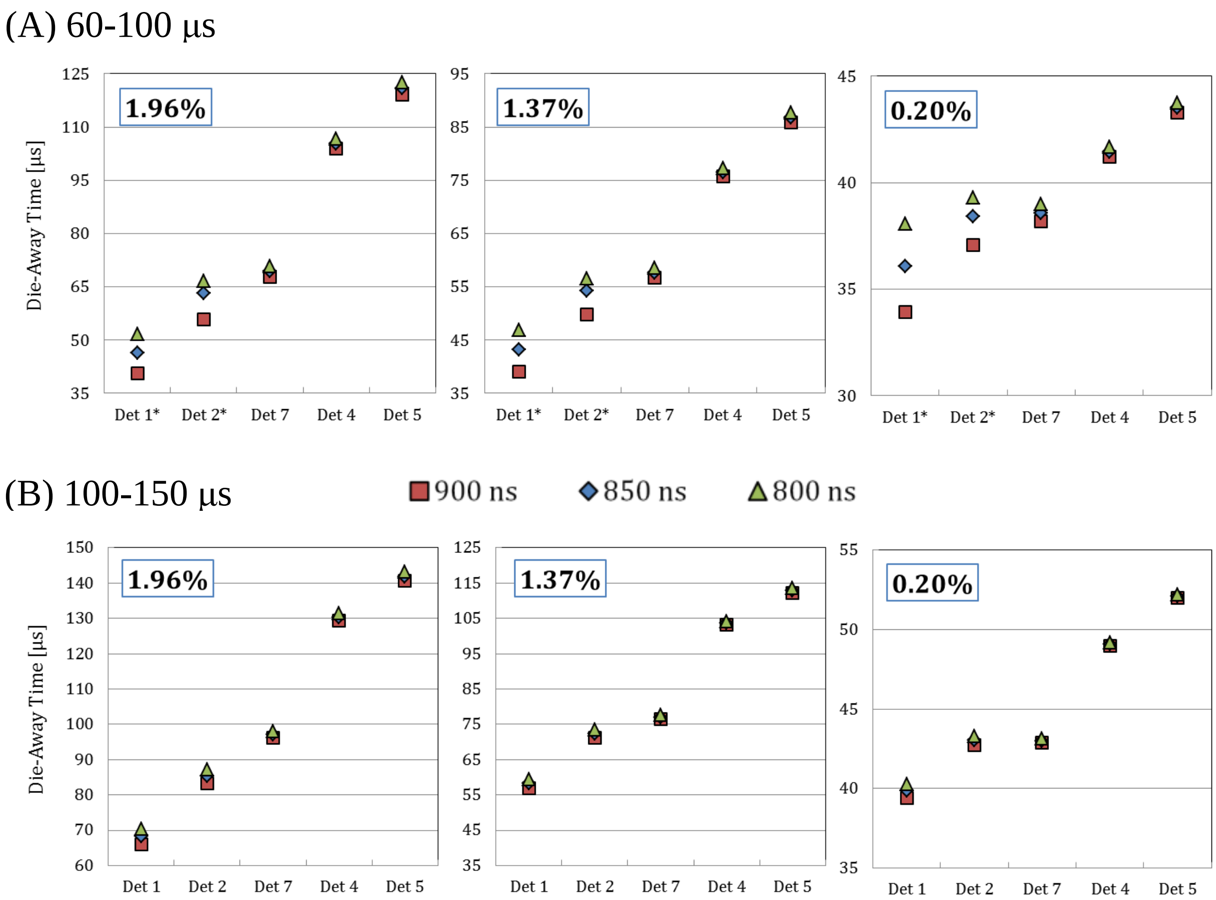

Figure 3. The die-away times in two time domains (A) 60-100 µs and (B) 100-150 µs for three different FFA enrichments (1.96%, 1.37%, and 0.20% ^{235}U) were calculated using different deadtime correction coefficients: 800, 850, and 900 ns. Detectors 1 and 2 were very sensitive to changes in the deadtime correction coefficient in the early time domain, with die-away time values ranging ±5 µs. In the later time domain, the detectors were not as dependent on the deadtime correction coefficient value.

IV. Fresh Fuel Simulations

4.1 MCNPX Simulation Setup

The DDA instrument setup in the simulations was designed to mimic the experimental setup as accurately as reasonably possible. The experimental setup is modeled in MCNPX with the fresh fuel assembly inside the water tank surrounded by three stainless steel detector pods containing a total of nine ^{3}He detectors (Fig. 4). The DT neutron generator is inside the waterproof stainless steel pipe inside of the water tank. Material definitions provided in a PNNL report [4] were used to define the materials in the simulation, as these definitions were previously verified.

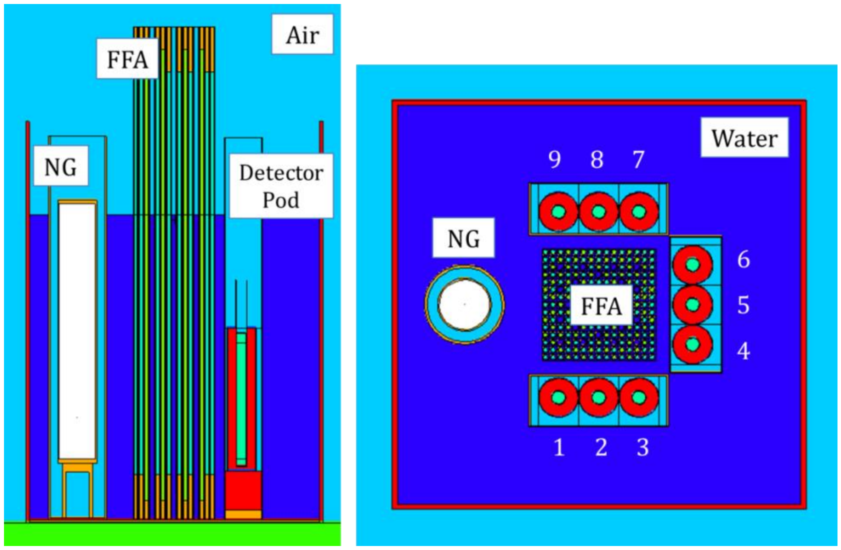

Figure 4. The MCNPX simulation for the fresh fuel DDA instrument models the experimental components realistically.

4.2 Sensitivity Studies

A variety of small changes to various parameters of the MCNPX simulation were investigated to determine their effect on the overall tally results. This simulation campaign allowed us to investigate small geometry discrepancies between the simulation and experiment, and to better understand the physics involved in the DDA technique. The simulations analyzed for this report included study of statistical variations in MCNPX results, the vertical source position of the DT neutron generator, varying the length of the inert regions of the fresh fuel rods, and the neutron generator pulse wrap-around effects.

4.2.1. Statistical Variation in MCNPX

In MCNPX, when identical input decks are run in the default mode, the tally results will be identical due to the problem being initiated with the same random number seed. The uncertainty on tallied quantities given by MCNPX is based on analysis of sub-sections of the calculation. However for quantities derived by post processing, such as die-away time, the statistical variation of individual MCNPX results can then be determined by analyzing values from identical problems but with different starting histories.

Five identical input decks with different starting histories were run for two cases: FFA with 1.96% ^{235}U enrichment and an empty assembly. The die-away time values for the nine detectors were determined based on the results of the simulations. The mean value and the standard deviation of the die-away times were determined for three different time domains: 0-50 μs, 100-150 μs, and 150-200 μs (Table III).

The die-away times changed marginally with different starting histories, with the 1.96% ^{235}U run more affected than the empty fuel assembly case. The back detectors, primarily Detector 5, experienced the largest deviation from the mean across the five runs. The relative error for all detector positions for both scenarios also increased as the time domain used to calculate the die-away time increased.

Table III

The standard deviation in the die-away time in three time domains was calculated from five MCNPX runs starting from different histories to determine the statistical variation in the results. The relative error increased in the later time domains. The back detectors were most affected by statistical variation in the transport code. The average and standard deviation values are in units of microseconds.

	Empty: DDA Signal Die-Away Time					
Time domain:	**50-100 μs**		**100-150 μs**		**150-200 μs**	
	Average	Std Dev	Average	Std Dev	Average	Std Dev
Detector 1	35.2	0.2	33.1	0.3	32.6	0.2
Detector 2	35.4	0.1	32.7	0.4	33.4	1.0
Detector 3	35.2	0.1	33.4	0.4	32.6	0.6
Detector 4	35.2	0.1	33.0	0.6	33.1	1.1
Detector 5	35.3	0.4	33.2	0.9	33.2	0.9
Detector 6	35.2	0.2	32.8	0.4	32.5	0.8
Detector 7	35.4	0.2	33.2	0.2	33.9	0.6
Detector 8	35.2	0.1	32.9	0.2	33.3	0.4
Detector 9	35.2	0.1	33.1	0.1	33.0	0.5

	1.96% ^{235}U: DDA Signal Die-Away Time					
Time domain:	**50-100 μs**		**100-150 μs**		**150-200 μs**	
	Average	Std Dev	Average	Std Dev	Average	Std Dev
Detector 1	46.6	0.2	60.2	0.4	90.6	1.1
Detector 2	55.3	0.2	75.4	0.5	112.5	1.3
Detector 3	59.2	0.4	85.6	1.2	125.4	3.7
Detector 4	79.9	0.8	118.6	0.9	156.0	4.1
Detector 5	88.5	1.9	138.6	2.9	165.9	6.4
Detector 6	79.7	1.2	121.8	3.8	161.9	4.9
Detector 7	59.3	0.3	85.7	1.7	124.8	4.3
Detector 8	55.0	0.2	75.7	0.6	113.4	3.7
Detector 9	46.7	0.2	60.3	0.4	90.7	0.7

4.2.2. Neutron Generator Vertical Source Position

The DT neutron generator target plane is marked on the actual accelerator tube. However, we were interested in determining if there was a significant sensitivity in the results due to the vertical position of the neutron source with respect to the rest of the experimental setup. Four MCNPX input decks were created with the NG target plane at different positions: 26 cm, 28 cm, 30 cm, and 32 cm above the water tank floor. The die-away times in two time domains for Detectors 1 and 5 were determined for three different fuel enrichments (1.96%, 1.08%, 0.49% ^{235}U) and an empty fuel assembly (Fig. 5). Overall, the effect of small changes to the NG source position on the die-away time seems rather negligible. The variation of the die-away time is within 2 μs and the results do not yield any systematic trends. This suggests that the variation of the die-away times is entirely due to the statistical fluctuations of the MCNPX results.

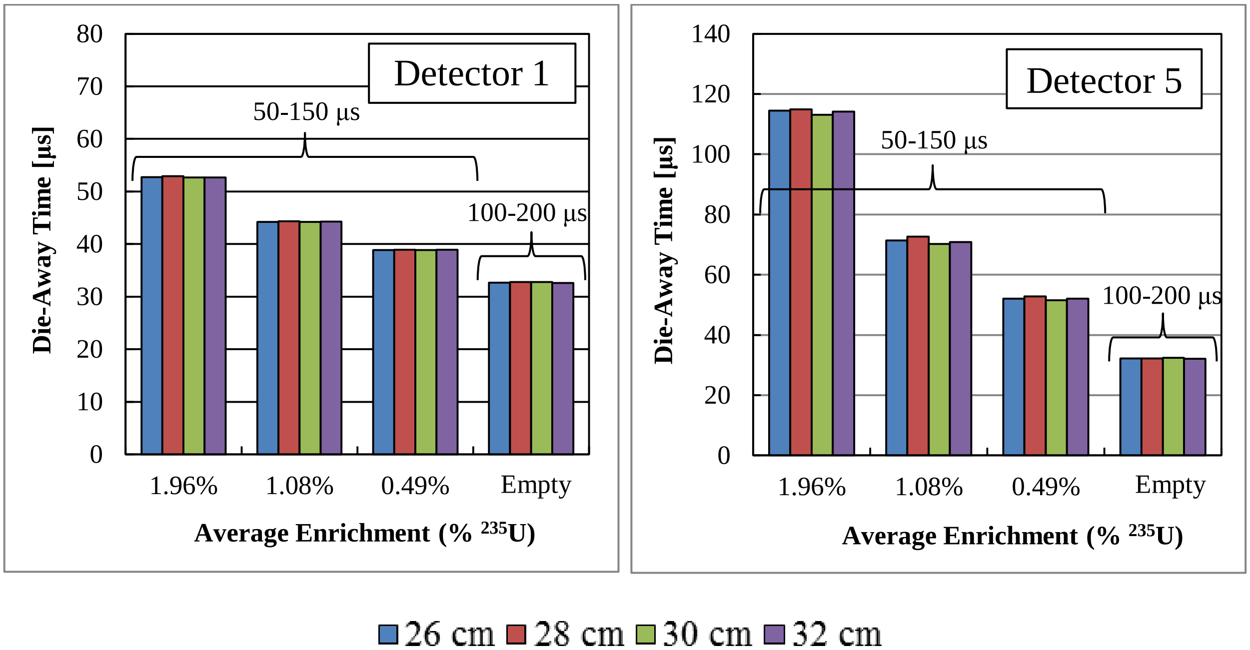

Figure 5. The vertical position of the neutron generator was simulated at four different heights (26, 28, 30, and 32 cm) to determine the effect on the DDA die-away time in the 50-150 μs or 100-200 μs time domains. The change in source height did not significantly affect the die-away time of the DDA signal.

4.2.3. Fresh Fuel Inert Regions

We investigated the effect of the inert regions at the top and bottom of the LEU and DU fresh fuel rods through a suite of MCNPX simulations. Three fresh fuel models were created and compared: (1) no inert regions, (2) 12 cm of stainless steel on bottom of LEU rods and 5 cm of stainless steel on bottom of DU rods, and (3) 20 cm of stainless steel on bottom of LEU rods and 10 cm of stainless steel on bottom of DU rods (Fig. 6). The inert stainless steel regions of the fuel decreased the overall amount of fissile material in the fuel rod, thereby affecting the die-away time of the DDA signal.

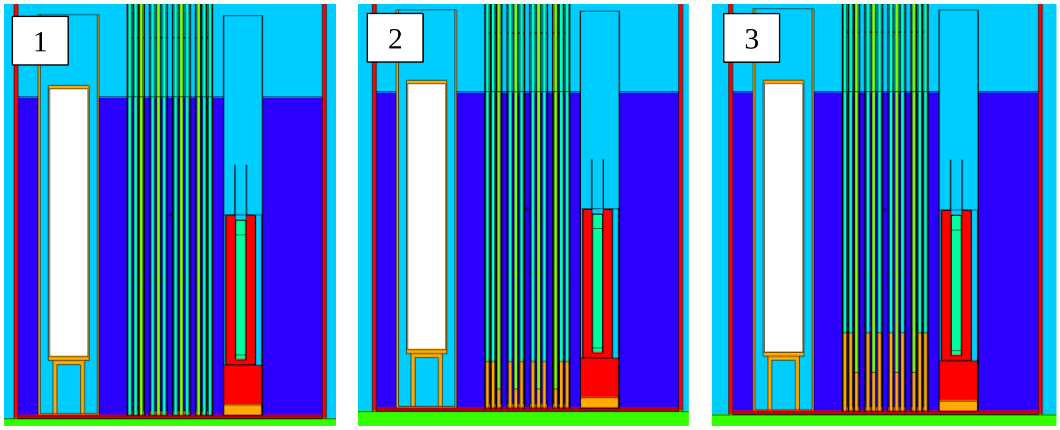

Figure 6. Three fresh fuel models were compared to determine the effect of inert fuel regions on the DDA signal. The models were (1) no inert region (original), (2) 12 cm of stainless steel on bottom of LEU rods and 5 cm of stainless steel on bottom of DU rods (fuel12), and (3) 20 cm of stainless steel on bottom of LEU rods and 10 cm of stainless steel on bottom of DU rods (fuel20)

The die-away time of the DDA signal in five detectors during the 100-150 μs time domain was calculated for four fuel enrichments: 1.96%, 1.37%, 0.79%, and 0.20% ^{235}U (Fig. 7). For all four enrichment cases studied, the die-away times for all detectors consistently decreased as the inert fuel region length increased. The effect more greatly impacted the higher enriched cases, with almost no effect to the depleted uranium (0.20%) case. As would be expected, the relative difference between the simulations of the original fuel (i.e. no inert regions) and the fuel with the inert regions increased as the inert region increased, reaching a level of 15-20% for the highest enriched case (Fig. 8). Also, the relative difference decreased as the average enrichment of the FFA decreased. The construction of the fuel rods is known sufficiently well that the contribution to the final error is negligible.

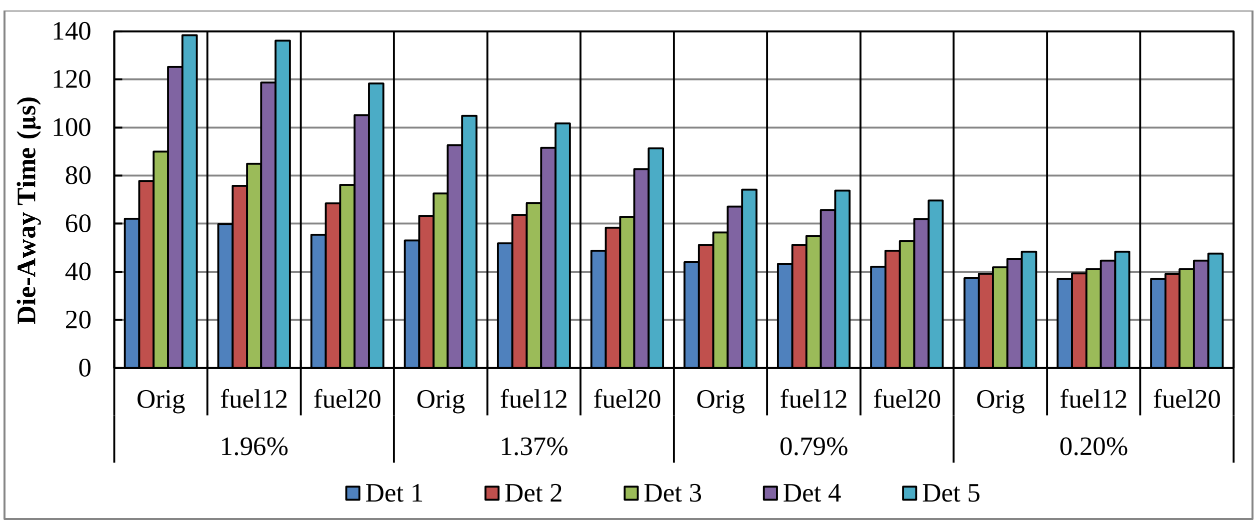

Figure 7. Comparison of the die-away times of the DDA signal in five detectors during the 100-150 μs time domain calculated for four enrichment scenarios. As the inert region of the fuel increased, the die-away time magnitude gradually decreased.

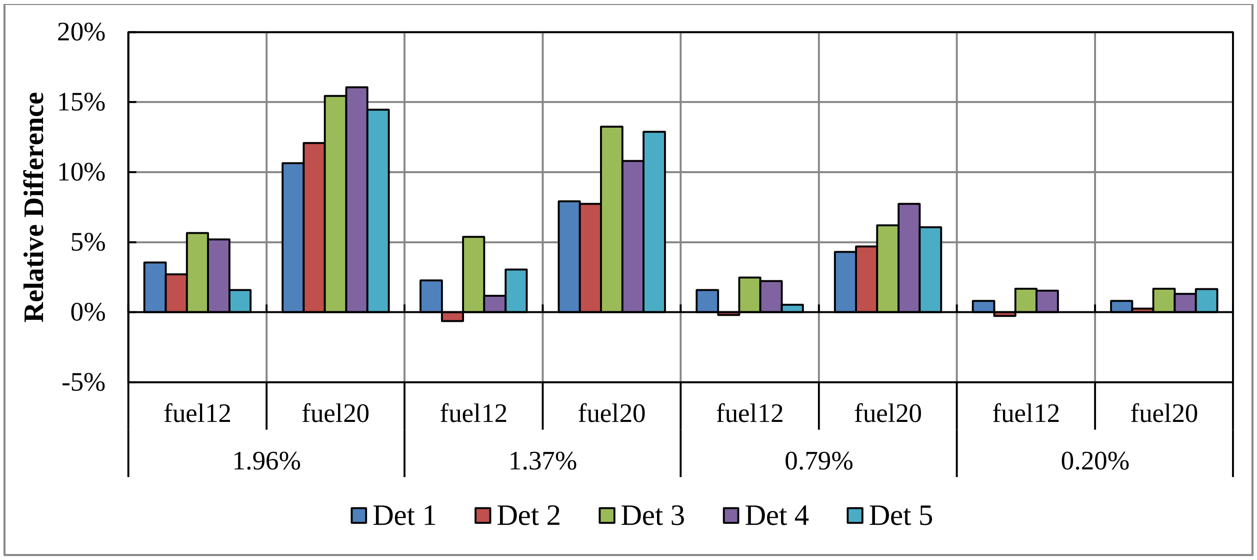

Figure 8. The comparison of the relative differences of the die-away times for the simulations with 12 cm stainless steel ("fuel12") and 20 cm of stainless steel ("fuel20") with respect to the original (no inert) fuel model. The relative difference between the die-away times increased as the inert region increased, peaking at ~15% for the highest enriched FFA scenario. As the average enrichment of the FFA decreased, the relative difference also decreased.

4.4.4. Neutron Generator Pulse Wrap-Around Effects

In MCNPX, only one neutron generator pulse is simulated per run. However, during an experiment, the neutron generator pulses tens of thousands of times as the data is acquired over many seconds. We investigated how neutrons from the previous pulse that may still be present in the fuel assembly or adjacent water regions could affect the die-away time determination, as this could contribute to possible differences between the experimental and simulated results.

During an experiment, we typically operate the DT neutron generator at 2500 Hz with a 20 μs pulse. Therefore, every 400 μs, a new pulse from the neutron generator interrogates the fuel assembly. The pulse wrap-around effects were imitated in simulation by summing the 0 μs and 401 μs tally values, 1 μs and 402 μs tally values, 2 μs with 403 μs tally values, etc., to account for the residual neutron population in and around the fuel when the next pulse occurs. As expected, the residual neutron population slightly increased the overall number of neutrons being detected in the simulation, thereby increasing the DDA signal and the magnitude of the die-away time (Fig. 9). On average, the pulse wrap-around effects increased the DDA die-away time magnitude by approximately 2% for all detector positions and enrichment scenarios, not including the empty FFA case (Fig. 10).

Another potential issue for future investigation is the influence of delayed neutrons. The delayed neutrons are technically included in the MCNPX simulation; however, the time cutoff of the neutron transport in individual neutron history simulation (1 ms), explicitly excludes them from the tally. However, in the experiment, as the neutron generator is turned on for up to several hours, we can expect that the rate of delayed neutrons might be saturated and contribute as constant background to the DDA signal. This would result in a slightly higher (approximately a few percent) die-away times, similar or perhaps even larger than the pulse wrap-around effects.

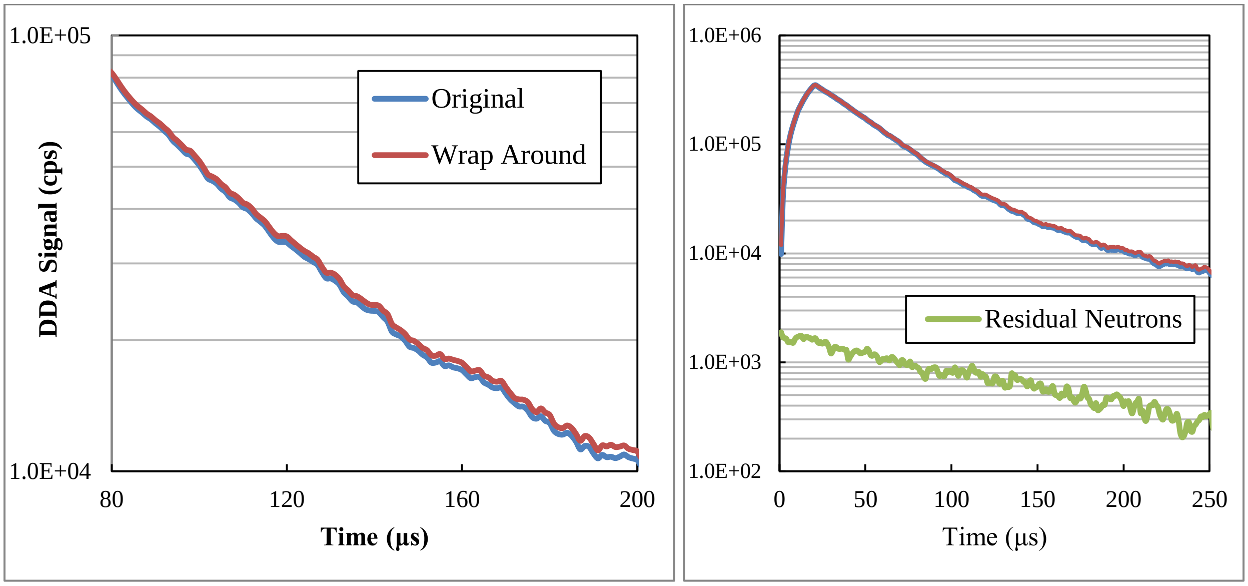

Figure 9. (Left) The simulated DDA signal from a single MCNPX simulation ("Original") was compared to the previous pulse wrap around effects included signal ("Wrap Around") from Detector 5. (Right) The magnitude of the residual neutron population from the previous pulse ("Residual Neutrons") was compared to the DDA signal magnitudes.

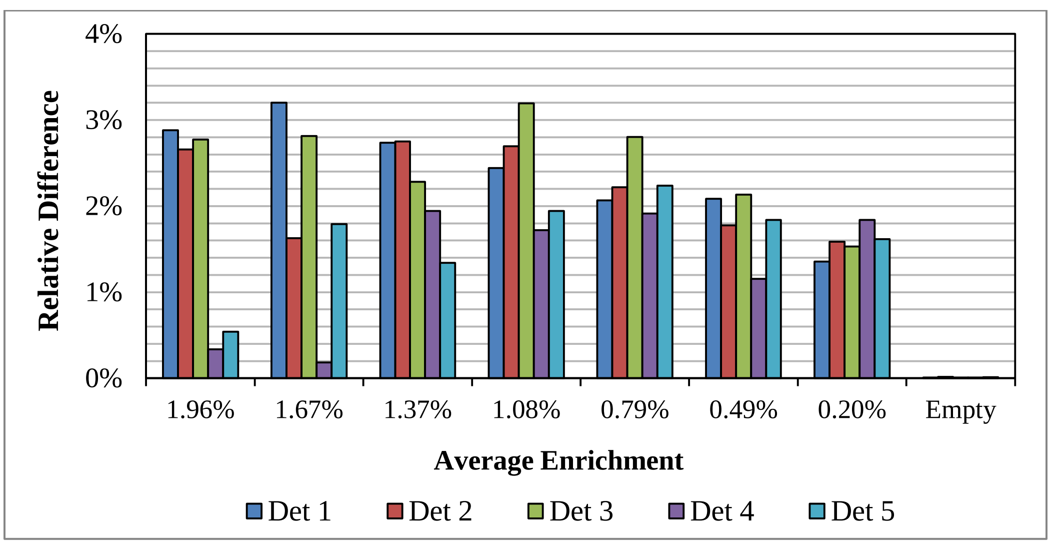

Figure 10. The relative differences between the simulated DDA signal die-away times of the original setup and the one including the wrap-around effects as function of the average FFA enrichment and the detector position. The wrap around die-away time magnitude was consistently larger than the original, due to neutrons lingering in the vicinity of the detectors. The empty FFA die-away time was not affected by pulse wrap-around effects.

One potential way to reduce the effect of the previous pulse neutrons is to insert sheets of Cd in the water around the FFA. Then if neutrons were to scatter into the water region and thermalize, they would be absorbed by the Cd and unable to re-enter the FFA and contribute to induced fissions in a later time domain. We may investigate this modification of the experimental setup in the future.

4.3 Simulation of the DDA Signal

Based partly upon the results from the sensitivity study, a series of MCNPX simulations that best exemplified the updated experimental geometry were compared. We compared results of three dedicated MCNPX simulations that encompassed our best understanding of the experimental setup: (1) fresh fuel with no inert regions, (2) fresh fuel with 12 cm of inert region at bottom of LEU rods and 5 cm of inert region at bottom of DU rods, and (3) fresh fuel with 12cm/5cm inert regions including neutron generator pulse wrap-around effects.

Using an estimated neutron generator yield of $1.8 \cdot 10^8$ n/s (± 5%), we compared the simulated DDA signals from Detectors 1,2,7,4 and 5. (Note: detectors in positions 3 and 7 are symmetrically positioned around the FFA and should thus register statistically identical count rates.) As seen in the plots in Fig. 11, the magnitude of the DDA signal changes slightly for the different MCNPX simulations for multiple fresh fuel enrichment scenarios. The “No Inert” (red) DDA signal consistently has a higher magnitude than the “12 cm Inert” (blue) DDA signal, due to the difference in the amount of fissile material in the fuel rods in the region near the detectors. This trend is also reflected with the different enrichment scenarios; as the amount of ^{235}U increases, so does the difference in the DDA signal magnitude between the “No Inert” and “12 cm Inert” simulations. The magnitude of the “12 cm Inert + Wrap-Around” (green) signal lies in between the two other cases. This highlights how the residual neutrons from the previous pulse contribute to the number of detected neutrons during the subsequent pulse, but do not fully offset the loss of fissile material due to the inert region of the fuel.

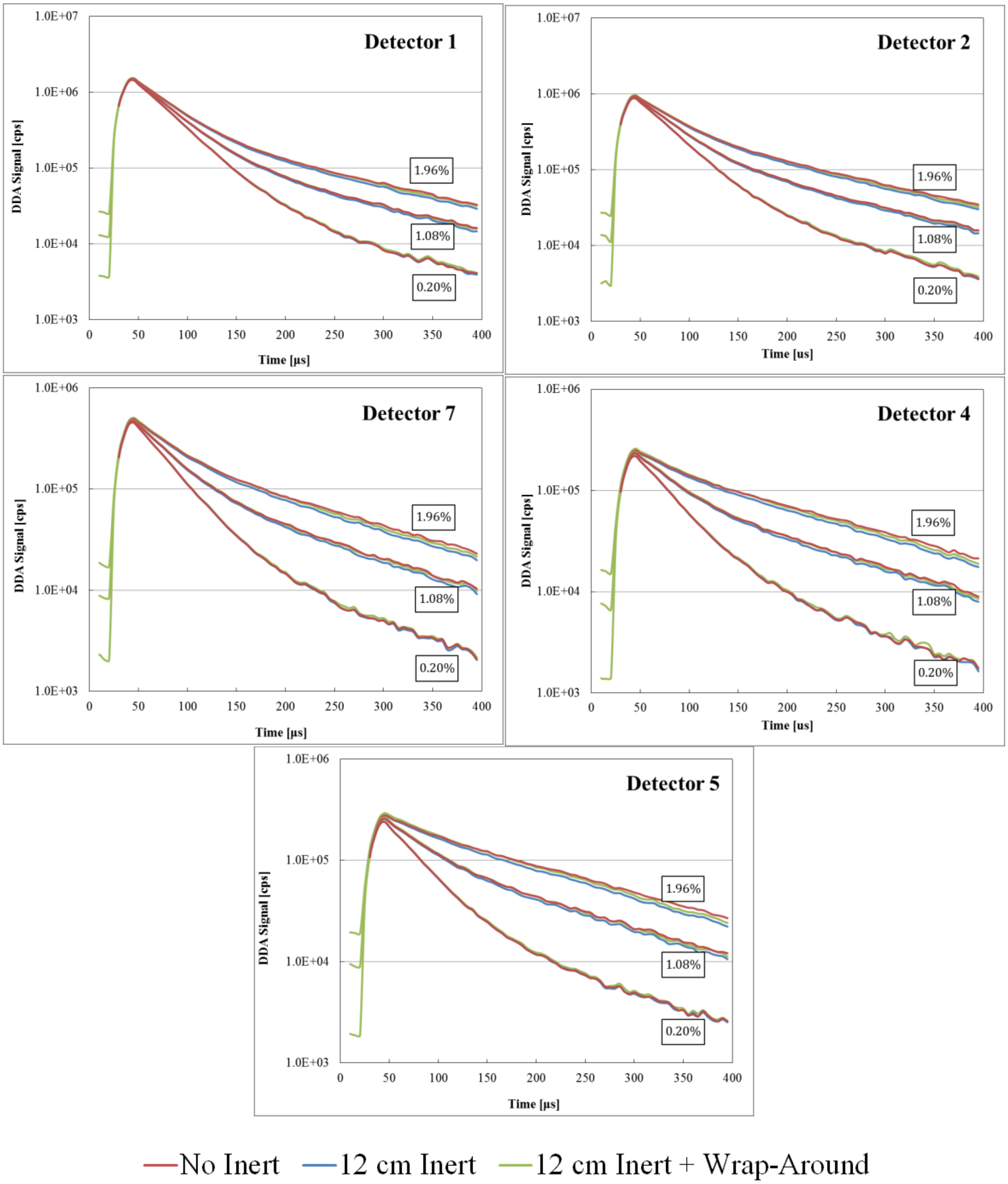

Figure 11. The DDA signals for 5 detector positions from three DDA models for three fresh fuel enrichments (1.96%, 1.08%, and 0.20% ^{235}U) were compared to determine the effects of fissile material quantity and previous neutron generator pulse wrap-around effects on the signal magnitude. The magnitude of the signal increased with increasing fissile mass in the fuel rods. Also, the 12 cm Inert + Wrap-Around effects increased the signal magnitude, but not to the level of the No Inert region simulation.

V. Comparison of Experiment and Simulation

The experimental and simulated results were compared to determine how accurately we can model and replicate the results from the complex DDA instrument using MCNPX. From both experiment and simulation, we evaluated several observables of the DDA instrument, such as the time-dependent behavior of the DDA signal, the DDA signal die-away time in two time domains, and the integral of the DDA signal in two time domains.

By examining the fresh fuel rods and assessing the MCNPX fuel sensitivity study, we determined that the "12 cm Inert + Wrap-Around" MCNPX simulation is so far the most physically accurate model to compare with the experimental results. By comparing the DDA signal magnitude from the simulation results to the experimental data, the DT neutron generator yield was estimated to be $1.8 \cdot 10^8$ n/s ± 5%. We used an experimental deadtime correction coefficient of 850 ns. Both the experimental and simulated data were acquired in 5 μs bins; the DDA signals were then converted to counts per second.

5.1 Dynamic Evolution of the DDA Signal

As seen in Fig. 12, the experimental (teal) time-dependent DDA signal is plotted with the "12 cm Inert + Wrap-Around" (green) MCNPX simulation results. Overall there is fairly good agreement between the simulation and experiment DDA curves for multiple enrichments and detector positions.

Detector 1 is heavily impacted by deadtime directly after the neutron generator pulse. This deadtime effect is due to the very high count rate experienced by the detector and its electronics. The count rates are so high that the deadtime correction model fails, giving rise to these signal excursions. We intend to upgrade our experimental detector/electronics packages by using LANL-made fast post-burst recovery electronics packages to improve the quality of the data at these early times.

Uncertainty in the DT neutron generator yield and small geometry discrepancies between the simulation and experiment would affect the relative magnitude of the DDA signal. These uncertainties may explain the small differences in magnitude for several of the comparisons, including Detector 7 with 0.20% ^{235}U and Detector 4 with 1.96% ^{235}U. The DDA signals from Detectors 2 and 5 appear to be particularly well matched.

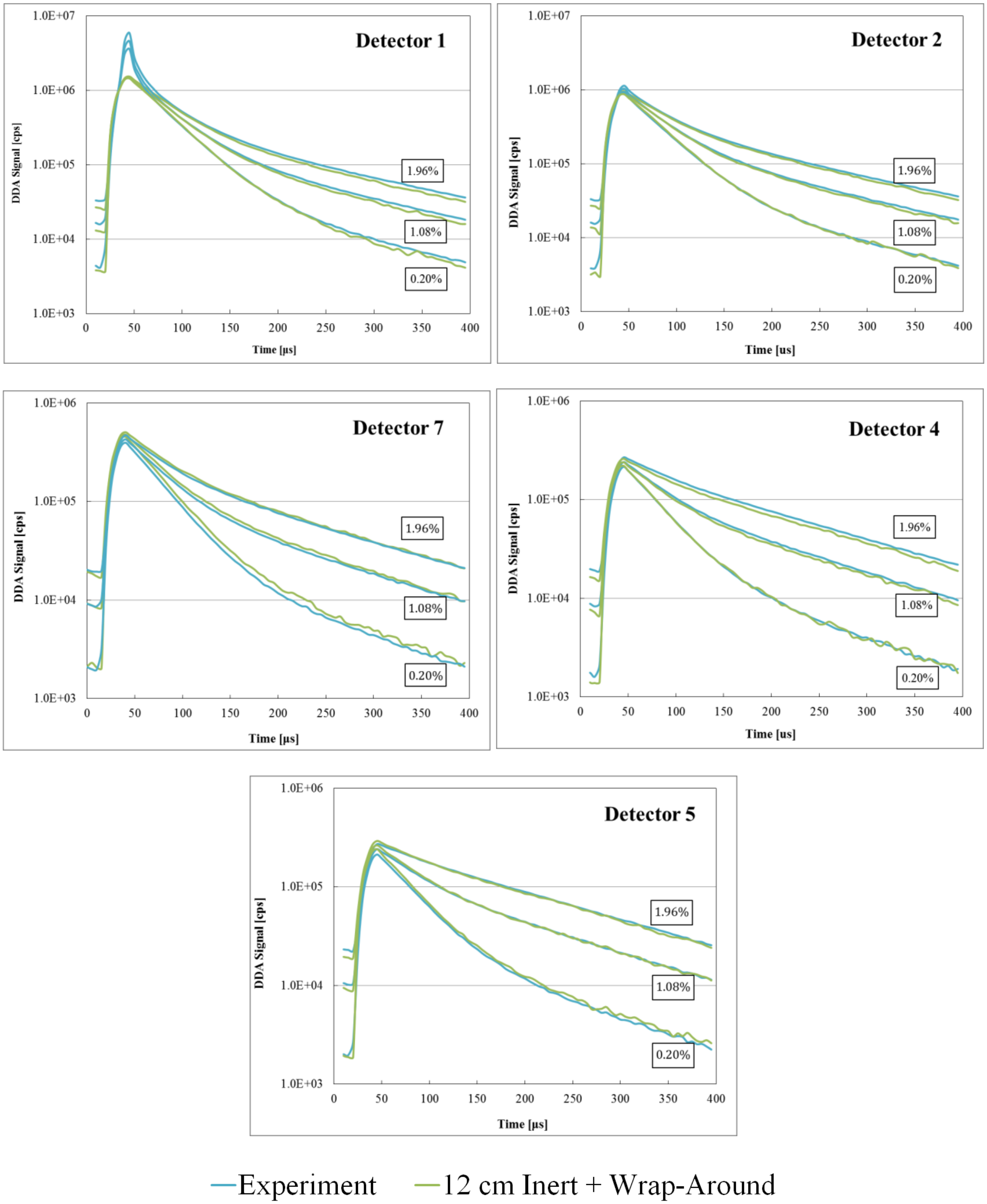

Figure 12. The dynamic evolution of the DDA signal is plotted for three fresh fuel enrichments.

5.2 Enrichment versus Die-Away Time

The experimental and simulated die-away times of the DDA signal were determined for two time domains: 60-100 μs (70-100 μs for Detector 2) and 100-150 μs. As seen in Figures 13A and 13B, the experimental and simulated die-away time versus average FFA enrichment were plotted and compared. For this comparison, we applied a 900 ns deadtime correction coefficient and estimated DT neutron generator yield of $1.8 \cdot 10^8$ n/s.

In the early time domain (60-100 μs, 70-100 μs for Detector 2), the experimental die-away times of Detectors 2, 7, 4, and 5 compare fairly well with the "12 cm Inert + Wrap-Around" MCNPX simulation die-away times. Detector 2 is particularly sensitive to deadtime correction in the early time domain due to the extremely high count rates registered by the front positions (closest to the DT neutron generator). The die-away times for Detectors 7, 4, and 5 compare well for all average FFA enrichments. The experimental die-away times of Detector 4 were consistently higher than modeled possibly due to a small geometry difference between simulation and experiment. If Detector 4 had been positioned slightly closer (approximately 1 cm) to Detector 5 in experiment, this would account for slightly elevated die-away times.

We also found good agreement between the experimental and simulated die-away times in the later time domain (100-150 μs). Generally, the experimental die-away times were slightly larger than the simulated values (Fig. 13B). This could be due to a small geometry error or slightly underestimating the fissile content in the fuel rods which would decrease the multiplication of the system and thus the detector die-away times. Through previously performed simulations [5], it has been shown that the back detectors are particularly sensitive to the total fissile content in the fuel assembly.

(A) 60-100 μs

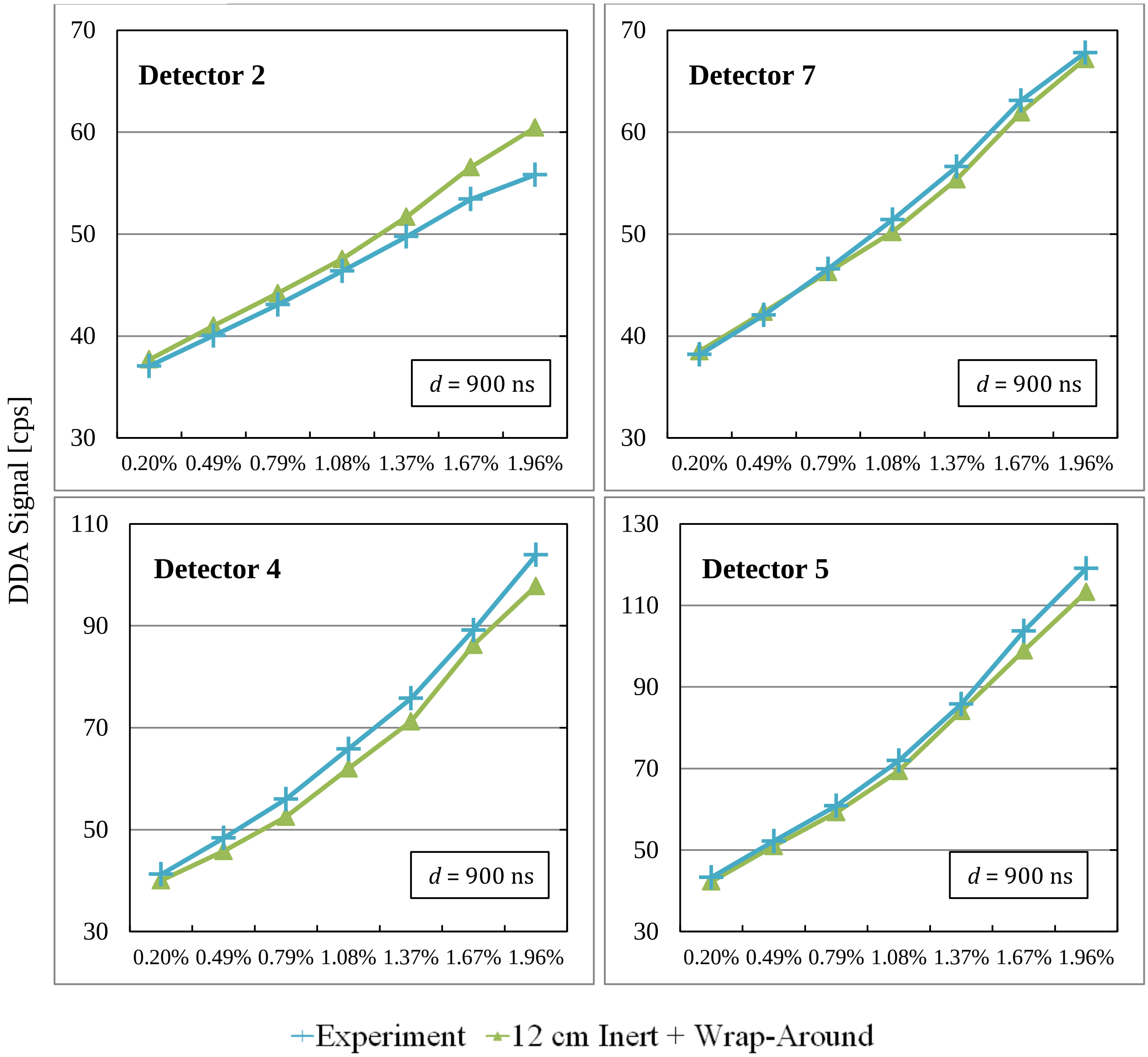

Figure 13A. The experimental and simulated die-away times of the DDA signal in the 60-100 μs (70-100 μs for Detector 2) time domain for seven FFA enrichments were compared. The experimental deadtime correction coefficient was set as 900 ns and the neutron generator yield was estimated as $1.8 \cdot 10^8$ n/s ± 5%.

(B) 100-150 μs

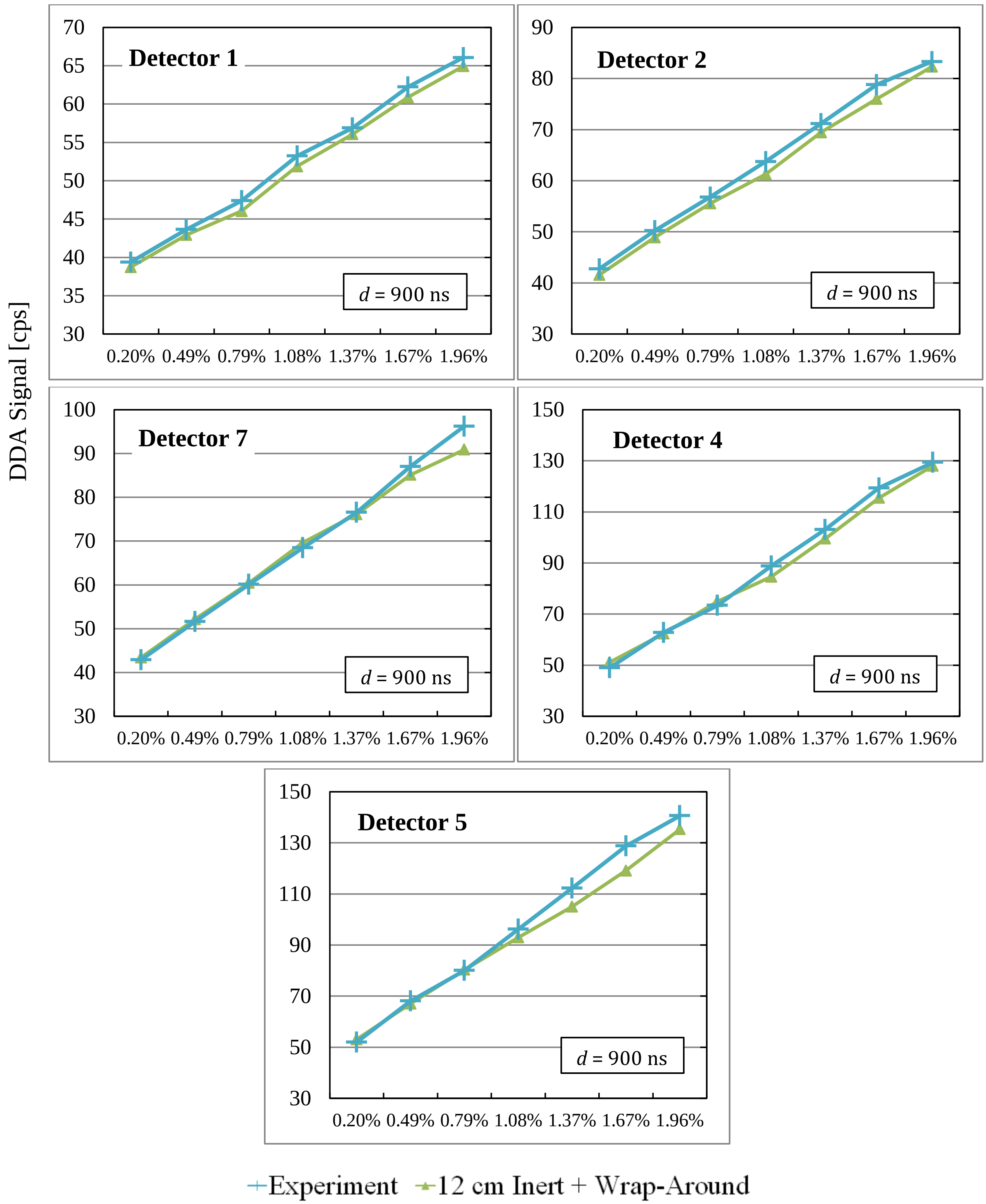

Figure 13B. The experimental and simulated die-away times of the DDA signal in the 100-150 μs time domain for seven FFA enrichments were compared. The experimental deadtime correction coefficient was set as 900 ns and the neutron generator yield was estimated as $1.8 \cdot 10^8$ n/s ± 5%.

We found fairly good agreement between the experimental and simulated die-away times both in terms of the trend with the average enrichment of the FFA as well as the absolute values. In the early time domain (60-100 μs), the experimental DDA signals from Detectors 1 and 2 were still recovering from the DT neutron generator burst which impacted the die-away time calculation. However, the die-away times from the three other detectors compared well with the simulated results, with an average relative difference of approximately ±2.9% (Fig. 14A). In general, the MCNPX simulations consistently underestimated the DDA signal die-away time. This could be due to a small geometry error.

In the early time domain, Detector 4 repeatedly had the largest relative difference between experiment and simulation for almost all of the enrichment scenarios. This may have been due to an irregularity with the detector electronics, the HDPE cylinder thickness, or a small geometry error. In addition, the relative difference in the early time domain appears to increase as the amount of fissile material in the FFA increases.

In the later time domain, Detector 5 had the largest relative difference between experiment and simulation, appearing to increase with average FFA enrichment. The average relative difference for all detectors and enrichments in the 100-150 μs time interval was approximately ±2.5%. From the mainly positive relative difference values, this shows that the simulation generally underestimates the DDA die-away time.

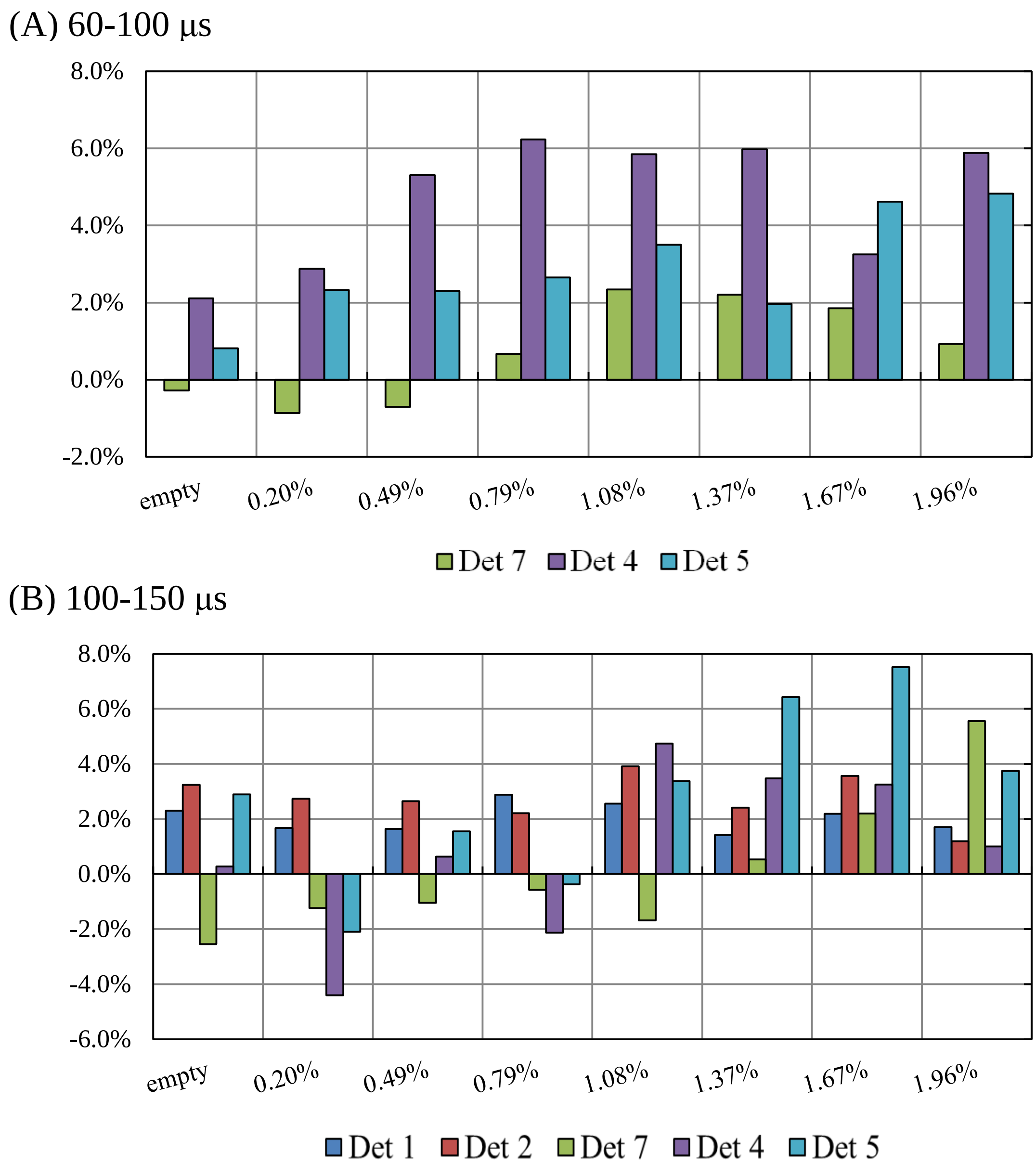

Figure 14. (A) In the early time domain (60-100 µs), the die-away times as a function of average FFA enrichment from Detectors 7, 4, and 5 compared fairly well with the simulated results, with an average relative difference of approximately ±2.9%. (B) In the later time domain (100-150 µs), the die-away times as a function of average FFA enrichment from all detectors compared well with the experimental results, with an average relative difference of approximately ±2.5%.

5.3 Integral DDA Signal

We integrated the DDA signal in the early (60-100 µs) and later (100-150 µs) time domains to compare the experimental and simulated values. In addition to depending on the amount of fissile material in the fuel, the magnitude of the DDA signal depends on the deadtime correction coefficient and the estimated DT neutron generator yield, both of which have uncertainties in their values. In this study, we used a deadtime correction coefficient of 850 ns and a DT neutron generator yield of $1.8 \cdot 10^8$ n/s ± 5%.

Overall, the average relative differences for the different detectors and fresh fuel enrichment scenarios ranged from ±4-10% (Table IV). Detectors 7 and 5 had the largest relative differences between the experimental and simulated values, especially for the empty FFA case. The larger relative differences between the integrals of the experimental and simulated DDA signals were likely due to uncertainty in the DT neutron generator yield or small geometry differences between the experiment and simulation.

Table IV

The relative differences between the experiment and MCNPX simulation (12 cm Inert + Wrap-Around) integrated DDA signal in an early (60-100 µs) and later (100-150 µs) time domain were determined.

	Integral DDA Signal 60-100 µs: Relative Difference				
	Detector 1	Detector 2	Detector 7	Detector 4	Detector 5
1.96%	5.4%	3.1%	-6.1%	7.8%	-1.8%
1.08%	1.8%	0.7%	-9.8%	4.1%	-4.3%
0.20%	-1.8%	-3.9%	-13.5%	-0.4%	-8.3%
Empty	-2.4%	-5.7%	-16.4%	-4.8%	-14.4%

	Integral DDA Signal 100-150 µs: Relative Difference				
	Detector 1	Detector 2	Detector 7	Detector 4	Detector 5
1.96%	4.6%	4.4%	-5.4%	9.1%	1.6%
1.08%	2.5%	3.7%	-9.7%	5.9%	-1.2%
0.20%	-0.4%	-2.0%	-15.5%	0.3%	-6.7%
Empty	-1.8%	-4.2%	-18.2%	-6.2%	-12.2%

VI. Discussion

6.1 Possible Explanations for Discrepancies

Overall, we found fairly good agreement between the experiment and simulations. However there is still a potential for rather small discrepancies not accounted for in the simulations. These include uncertainty in the DT neutron generator yield, simplifications or uncertainty in the material definitions, and relatively minor differences in geometry between the experimental setup and its model in MCNPX. There is also uncertainty in deadtime correction coefficient value which, however, would affect primarily only the front detectors in the early time domain.

6.2 Areas for improvement

We plan to continue performing experiments and simulations of the fresh fuel DDA instrument. In subsequent experimental campaigns, we will upgrade our detector/electronics packages to faster post-burst recovery systems. This will decrease the deadtime and thus the magnitude of the necessary deadtime corrections and allow for analysis of the DDA signal closer to the DT neutron generator peak.

VII. Conclusions

The DDA instrument is undeniably a measurement system capable of capturing the complex time-dependent signal that contains a wealth of information about the assayed item. Through the experiments and simulations described in this report, we have demonstrated that MCNPX can provide reliable results, which supports the promising conclusions from previous simulation work that the DDA technique is suitable for spent fuel measurements [6] and further improved our understanding of the DDA technique, as well as demonstrating the practical aspects of neutron generator use and data collection and analysis.

VIII. Future Work

During the next three quarters, we plan to perform experiments and corresponding simulations of:

(1) The influence of neutron poisons present in the FFA in form of gadolinium fuel rods to mimic the presence of neutron absorbers in spent fuel,
(2) Various pin diversion scenarios, and
(3) Procure a set of LANL-made fast post-burst recovery KM200 packages for further testing and improvement of the DDA instrument's performance.

IX. References

[1] A. Goodsell, M. Swinhoe, V. Henzl, K. Ianakiev, M. Iliev, C. Rael and D. Desimone, "Differential Die-Away Instrument: Report on Neutron Detector Recovery Performance and Proposed Improvements," LA-UR-14-27369, Los Alamos, 2014.

[2] K. Ianakiev, M. Swinhoe, M. Iliev and A. Goodsell, "New-Generation Thermal Neutron Detectors and Electronics for High-Count Rate Applications," LA-UR-14-23377, Los Alamos, 2014.

[3] AMPTEK, "A111 Charge Sensitive Preamplifier & Discriminator," AMPTEK, [Online]. Available: http://www.amptek.com/products/a111-charge-sensitive-preamplifier/. [Accessed September 2014].

[4] R. McConn, C. Gesh, R. Pagh, R. Rucker and R. Williams III, "Compendium of Material Composition Data for

Radiation Transport Modeling," PNNL-15870 Rev. 1, Richland, 2011.

[5] T. Martinik, V. Henzl, S. Grape, S. Jacobsson Svard, P. Jansson, M. Swinhoe and S. Tobin, "Simulation of Differential Die-Away instrument's response to asymmetrically burned spent nuclear fuel," *submitted for publication in Nuclear Instruments and Methods in Physics Resarch A,* 2014.

[6] V. Henzl, M. Swinhoe, S. Tobin, H. Menlove, J. Galloway and D. Won Lee, "Direct Measurement of Initial Enrichment, Burn-up and Cooling Time of Spent Fuel Assembly with a Differential Die-Away Technique Based Instrument," in *Institute of Nuclear Materials Management*, Orlando, 2012.